Making an Enhanced Map for Lane Location Based Services

D Bétaille, R Toledo-Moreo, J Laneurit

Proceedings of the 11th International IEEE Conference on Intelligent Transportation Systems Beijing, China, October 12-15, 2008

Making an Enhanced Map for Lane Location Based Services

D. Bétaille, R. Toledo-Moreo and J. Laneurit

***Abstract*— Latest investigations show the benefits of fusing map information with GNSS (Global Navigation Satellite System) and dead-reckoning measurements for road vehicle navigation. However, to achieve success enhanced maps (Emaps) that take into account this new capability must be developed. In this paper, we present a method to create an Emap that includes road shape information, capable to serve as an input of a combined Fusion/Map-Matching algorithm. Details of the processes of road segments extraction and connection are given in the text. The analysis of the results obtained using the proposed method and future guidelines conclude the paper.**

I. INTRODUCTION

Most geographical information systems (GIS) represent roads with polylines, i.e. series of nodes and shape points, connected by segments [1]. Nodes are different from shape points because they stand for either crossroads, or, in case of junctions, entrances or exits. Additionally, shape points provide a spatial sampling of the road they belong to, with a level of approximation that meets the requirements of navigation systems today in term of map rendering. Some Advanced Driver Assistance Systems (ADAS), such as flexible lane allocation, enhanced driver awareness, lane keeping, auto cruise control, cannot rely solely on this representation, for a couple of reasons that we can split into accuracy and completeness. Like any model, this representation partially corresponds to ground truth: road is simplified since only its centerline is mapped. Moreover, what is modelled has limited accuracy from global and local points of view:

- Globally: Many digital maps often show similar inaccuracy as paper versions: maps are not always exactly scaled, neither coherent from one "page" to another. Similar techniques (photogrammetry) are used for traditional cartography and digital, leading to similar drawbacks. The accuracy level of standard maps today is around 5 m (for metropolitan areas) up to several tens meters.
- Locally: road geometry is approximated by series of shape points. Therefore, the actual distance between a chord (i.e. a segment defined by two consecutive shape points) and the ground truth arc, may exceed 1 m in curves, even dramatically more in roundabouts, where one can find a simple node representation. A higher spatial sampling obviously would contribute to locally improve the modelling of road geometry, but this would make it impossible data storage and access in real-time vehicle implementation.

D. Bétaille is with the Laboratoire Central de Ponts et Chausses, LCPC Nantes Centre. R. Toledo-Moreo is with the University of Murcia, Dept. of Information and Communication Engineering. Jean Laneurit is with the Technical University of Compiegne. david.betaille@lcpc.fr, toledo@um.es, jean.laneurit@hds.utc.fr

As concerns completeness, we should emphasize the fact that standard digital maps representation highly simplifies road description. For a one-way road, a unique polyline is used, regardless its number of lanes, and a similar simplification applies to two-way roads where there is no separation between driving directions. To sum up, global and local errors, as well as missing contents, cause at least mis-map-matching, but also make it impossible applications at lane level accuracy. Despite a few information items have been added to standard road maps that partially fulfill the ADAS requirements, like the number of lanes (that can be stored as an attribute of road segments), or also the lanes widths, further progress is still needed. What the e-map suggests goes further both in term of accuracy and contents.

II. MOBILE MAPPING AND DATA COLLECTION

Mobile mapping is already a way of collecting directly road network geometry by circulating the area to map. Where the GPS coverage is sufficient, it has the main advantage of delivering the final result almost directly with no bias. In the eventuality of GPS outages, which is common in dense urban center, the vehicle position cannot be determined by GPS only. Odometry and inertial aiding offer an efficient improvement, with however possible bias due to inertial integration drift. Depending on the quality of the IMU (inertial measurement unit) as well as on the GPS coupling strategy (tight with any visible satellites pseudo-ranges, or loose with navigation solutions only), this drift may exceed - in case of long duration outage - the mapping requirements in term of accuracy. Algorithms for coupling GPS with IMU and odometry, with appropriate calibration of these instruments, provide reliable statistics to select doubtful areas. Further in this article, GPS+DR (that stands for dead-reckoning) will refer to vehicle location obtained by such coupling.

On a complex interchange area or in a city center, a comprehensive mobile mapping necessarily induces a certain redundancy in the data collection: some sections will be circulated twice or more, which requires manual cut at data processing. In addition, any eventual specific maneuvers made during the data collection have to be suppressed before their use for mapping. Depending whether or not a visual inspection of the itinerary is possible off-line (monitoring the images of a front camera vision for instance) the operator must not forget to log event markers whenever obstacles have to be avoided leading to a non-nominal trajectory.

Another interesting way of collecting data was investigated by US project EDMap (enhanced digital map) in

the beginning of the 2000th, based on the fusion of the trajectories given by a fleet of GPS equipped cars [2], [3]. This approach is known under the name "probe-data". Note that the analytical road representation that we suggest in the sequel of this paper is not dedicated to mobile mapping and it should be applied to other data collection.

III. ANALYTICAL ROAD REPRESENTATION

Instead of sampling spatially the trajectories with shape points, we suggest an alternative that consists in extracting analytical equations that best fit these trajectories. It is interesting to notice that road design consists, among other activities, in developing in 2D+1 (horizontal and vertical dimensions separately) series of straight lines, circles and clothoids horizontally, as well as straight lines and parabolas vertically [**?**], [4]. So that one may expect similar mathematical structure hidden in mobile mapping data. Straight lines, circles and clothoids all obey to the same curvilinear 2D equations, with constant curve as concerns the circle, null curve in the case of the line. In a Cartesian frame, these equations are functions of the curvilinear abscissa, i.e. the distance performed along the curve. These functions are not explicit but they are given under the form of the following Fresnel's integrals:

$$x(l) = x_0 + \int (cos(\tau_0 + \kappa_0 l + \frac{cl^2}{2})dl, \qquad 0 < l < L$$

$$y(l) = y_0 + \int (sin(\tau_0 + \kappa_0 l + \frac{cl^2}{2})dl, \qquad 0 < l < L$$

where:

- x_0 and y_0 are the initial co-ordinates of the curve,
- τ_0 is the initial bearing of the curve,
- κ_0 its initial curvature,
- c its curvature rate with the curvilinear abscissa $(d\kappa/dl)$ with $\kappa = \kappa_0 + cl$,
- l the curvilinear abscissa, and
- L the total length of the curve.

In order to provide applications with a comprehensive description of the road, each carriage way, and each lane, must be described by series of curves similar to the aforementioned mathematical structure. In a former release of our extraction process, we applied systematically similar computation to all lanes, regardless their usual parallelism. This way, singular change of road cross-section or lane width will not cause any trouble. The key point is to survey each lane, driving as close as possible to its center and as far as possible when it merges with another. Crossroads, despite they were covered during mobile mapping, have been removed from the scope of this geometrical representation, since they let too many trajectories possible.

A. EXTRACTION PROCESS

The determination of straight lines and circles among a sequence of surveyed points is efficiently solved with least squares: Newton-Raphson or Levenberg-Marquadt's methods can be applied in this context. However, we aim at fitting geometrical elements closer than 5 cm to the vehicle trajectory, which could lead to a large number of lines and circles. Moreover, geometrical transitions between the identified elements still remain difficult to achieve, since linking the extremities of consecutive straights lines and circles makes sudden discontinuities if no long enough clothoids are fitted between. As a consequence, we have given priority to these transitions in the extraction process, and, since clothoids have the advantage of the generic form (that degenerates into circles or lines zeroing one or two parameters) we will propose a clothoids-only extraction process.

Let us assume that the longitudinal geometry of a lane is a stochastic process, variable as a function of the performed distance along this lane, with a priori unknown parameters x_0, y_0, τ_0, κ_0 and c. This set of parameters encompasses either straight lines, circles or actually clothoids. With respect to this process, GPS (or GPS+DR) locations can be considered as observations. The dynamics of this process can be deduced from the Fresnel's integrals, with a second order Taylor's development, which cope with their non-explicit expression.

$$x(l + dl) = x(l) + cos(t)\ dl - 0.5 \cdot \kappa\ sin(t)\ dl^2$$

$$y(l + dl) = y(l) + sin(t)\ dl + 0.5 \cdot \kappa\ cos(t)\ dl^2$$

with

$$t = t_0 + \kappa_0 l + 0.5 \cdot cl^2 \quad \text{and} \quad \kappa = \kappa_0 + cl.$$

and dl denotes the elementary distance performed to compute the integrals. In the following, dl is considered as an input in the prediction process. We fixed its value at 1 cm. This process fits the state-space and Markovian chain representation suitable for Kalman filtering, with a vector composed of the main variable l plus the parameters to identify x_0, y_0, t_0, κ_0 and c, plus x and y resulting from the integration. For simplification and robustness purpose, x_0 and y_0 have not been included in the identification process, and their value will be fixed by the first GPS+DR observation. So in discrete representation, the prediction model is:

$$\begin{aligned}
l(k+1|k) &= l(k|k) + dl \\
\tau_0(k+1|k) &= \tau_0(k|k) \\
\kappa_0(k+1|k) &= \kappa_0(k|k) \\
c(k+1|k) &= c(k|k) \\
x(k+1|k) &= x(k|k) + cos(t)\ dl - 0.5 \cdot \kappa\ sin(t) dl^2 \\
y(k+1|k) &= y(k|k) + sin(t)\ dl + 0.5 \cdot \kappa\ cos(t) dl^2
\end{aligned}$$

with

$$\tau = \tau_0(k|k) + \kappa_0(k|k) l(k|k) + 0.5 \cdot c(k|k) l(k|k)^2$$

and

$$\kappa = \kappa_0(k|k) + c(k|k) l(k|k)$$

and the observation model is:

$$x_{GPS+DR} = x(k+1|k)$$
$$y_{GPS+DR} = y(k+1|k)$$

In matrix notation, this gives:

$$X = [\ l\ t_0\ \kappa_0\ c\ x\ y\ ]' \quad (1)$$

and P denotes its variance-covariance matrix. The prediction and observation models in matrix notation are:

$$\begin{aligned} X(k+1|k) &= f(X(k|k), U(k+1) + \nu_U) + \nu_{Mod} \\ U(k+1) &= dl \\ Y_{GPS+DR} &= \begin{bmatrix} 0\ 0\ 0\ 0\ 1\ 0 \\ 0\ 0\ 0\ 0\ 0\ 1 \end{bmatrix} X(k+1|k) + \nu_{GPS+DR} \end{aligned}$$

where ν_U, ν_{Mod} and ν_{GPS+DR} represent respectively the prediction, input and observation noise vectors. Both input and observation noise vectors are assumed to be normally distributed with means equal to zero. They are therefore characterized by their variance.

- Input variance: e.g. $Q = dl^2$ in m^2. With dl equal to 1 cm, the integration error between GPS points typically separated by a few meters will consequently have an order of magnitude of the decimeter (i.e. the square root of a few hundreds of elementary centimeter dl errors integrated). This progress of the error is comparable to the possible observation error below, which enable outlier detection.
- Observation variance: e.g. $R = 0.2^2 \cdot I(2)$ in m^2 in areas where fixed kinematic GPS solutions are available. Note that R should vary along with the a posteriori statistics of the GPS+DR fusion output.

The prediction error will be considered as negligible with respect to the integrated input error. So the prediction noise vector will be set to zero. Being f a non linear function, its jacobian matrixes Jf_X and Jf_U with respect to X and U will be computed and used to update P:

$$P(k+1|k) = Jf_X P(k|k) Jf_X' + Jf_U Q Jf_U'$$

EKF (extended Kalman filter) formulation gives the a posteriori variance-covariance matrix:

$$P(k+1|k+1) = \Big(I - P(k+1|k)H'\big(HP(k+1|k)^{-1}H' + R\big)H\Big)P(k+1|k)$$

After a few iterations, this state space system should converge onto a correct estimation of the geometrical parameters. The theory stands that minimum 4 observation points are required for a clothoid, alike 3 or 2 for a circle or a straight line. What this method cannot perform is the determination of several clothoids in the same process. In practice, clothoids have to be extracted one after the other, which makes it necessary regular reset of the filtering process. The conditions for stop and start clothoids will be now discussed.

B. CONDITIONS FOR DETECTING CLOTHOIDS TRANSITIONS

In statistical term, a transition should correspond to the violation of the hypothesis along which all consecutive points would belong to the same clothoid. The statistical test on the normalized innovation squared (NIS, also called Mahalanobis distance, where the innovation is the distance between the predicted point $[x(k+1|k), y(k+1|k)]'$ and the observed Y_{GPS+DR} solutions) that one applies to any new observation is necessary, but not sufficient is this extraction problem. Actually, this test is applicable to any new point since it can be considered as doubtful with regard to the current clothoid.

$$NIS = (Y_{GPS+DR} - HX(k+1|k))' \cdot \cdot\ (HP(k+1|k)H' + R)^{-1}(Y_{GPS+DR} - HX(k+1|k))$$

In a χ^2 test, this distance should be compared to a threshold that depends first, on the degree of freedom of the system, second, on the probability of non-detection that one accepts for this test. When a GPS+DR observation makes NIS exceed the χ^2 threshold, then a probable outlier has been detected. But in case this point is accepted, it is not presumable whether or not the new clothoid that includes this point should remain coherent with the previous observations. It therefore appears that a more complete test is required. So, after every estimation step, the new clothoid (that includes the very last accepted GPS+DR point) is checked as follows:

- the number of previous GPS+DR points that are further than 5 cm to this clothoid is computed,
- if this number exceeds 2, this means that the current GPS+DR point has shifted away the extracted clothoid: then, one invalidates the last observation update and one comes back to the predicted set of parameters before,
- another counter is incremented whenever the preceding test concludes to an invalidation, decremented otherwise
- when this counter exceeds 4, one considers that a new clothoid has started.

Actually, 4 is the minimum number of points needed to fit a clothoid. Then, a new clothoid has started. This entails a reset of the parameters contained in the state vector (and a registration of the latest validated parameters).

IV. EXPERIMENTAL VALIDATION

The sensors placed on board the mobile mapper were:

- a Zmax kinematic GPS receiver, logging at 10 Hz
- a KVH RD2100 fiber-optic single-axis gyrometer, used at 10 Hz
- an encoder mounted on the gearbox of the rear-wheel Ford van, with a step of 0.2615 m.

The same GPS receiver was set-up in the vicinity of the test site: the maximum length of the baseline between both receivers did not exceed 5 km. GPS data were post-processed with GNSS Solutions. The obtained navigation solutions were fused in an optimal Raugh smoother with the gyro and odometer data (GYROLIS) [5].

Figs. 1 and 2 illustrate, on the extraction of the first element, the invalidation of the observation update corresponding to the 36th GPS+DR point. When this point is introduced, it appears that the previous 11th and 12th locations are further than 5 cm to the current clothoid, though they passed through the NIS test before (which makes sense because they are actually not outliers). Fig. 3 displays the predicted

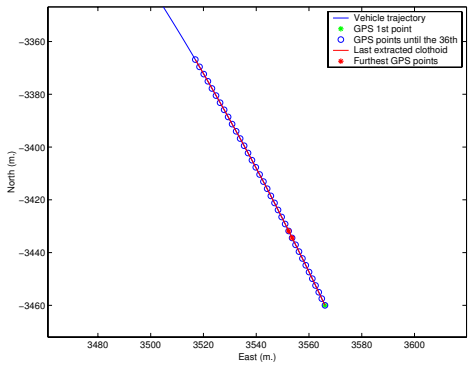

Fig. 1. Extracted clothoid (solid red) using the 36 first points. When introducing the 36th point of the GPS+DR trajectory (solid blue), two previous points that deviate from the clothoid by more than 5 cm appear.

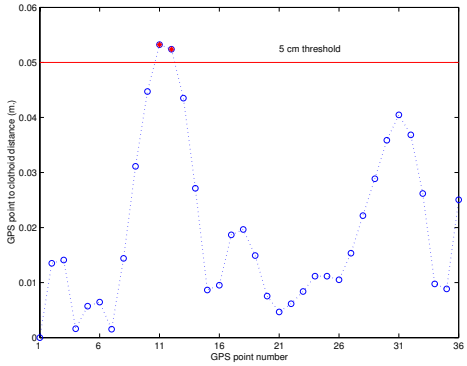

Fig. 2. Residual distance between the last extracted clothoid and the 36 first GPS + DR points used for its extraction. The 5 cm threshold is exceeded by two points, which indicates that a new clothoid should start.

standard deviations of the six state vector components of (1) until the 36th GPS+DR observation. Fig. 4 shows the series of clothoids extracted from a GPS+DR trajectory of our mobile mapper in a loop of the Cheviré bridge south interchange.

V. CONNECTION OF ROAD SEGMENTS

Despite the fact that segments could be connected manually, the convenience of an automated procedure to associate road segments is clear. Therefore, we decided to develop an automated algorithm to find those road segments to which it is possible to make a transition from a known one, presented in this Section. In its development, computational considerations were taken into account to avoid excessive time in the preparation of the connectivity map. Nevertheless, all processes can be executed a priori and off-line, and therefore no sharp restrictions in terms of computational time were established. For the case of the Emap of Cheviré bridge, with 553 segments and 1694 connections, this process requires less than 2 hours in a dual core laptop at 1.67 GHz running in Matlab, and using only one CPU for this process.

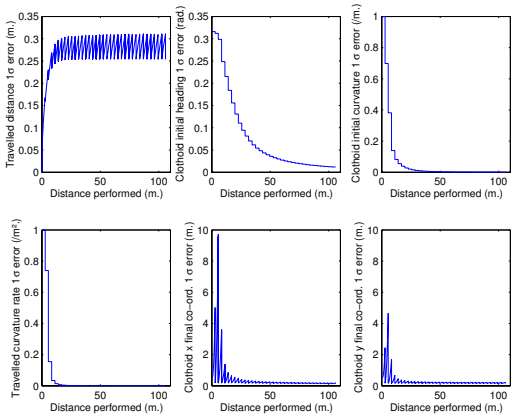

Fig. 3. Standard deviations output by the EKF. They apply to the 6 components of the state space vector. In the prediction/estimation process, standard deviations increase at prediction, decrease at estimation, which explains the pattern in the figures. The clothoid parameters progressively converge while additional GPS+DR points are included.

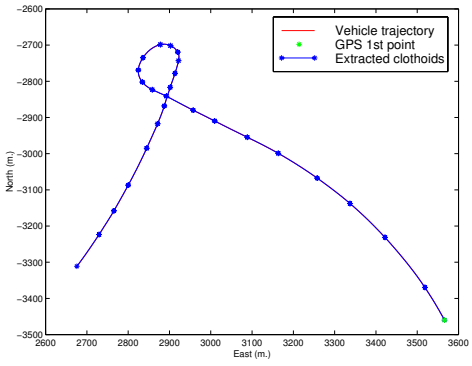

Fig. 4. Extract of the final Emap (one lane only is shown here). The vehicle trajectory (solid red) is hidden by the series of clothoids (solid blue) at the scale of this figure.

A. NUMBER AND DEFINITION OF NEIGHBOR SEGMENTS

Our task entails finding those road segments in which the vehicle could be, when it will leave the current one. In that way, the connectivity concept as defined in our approach is not bijective and will have a concrete direction. Therefore, it can be found feasible to make a transition from segment F to segment I, noted as $F2I = 1$, but not from I to F ($I2F = 0$). This orientation feature suits well to the traffic restrictions of single direction lanes. Fig. 5 shows an example of this case. For the Emap of Cheviré bridge developed in the area of Nantes, 553 road segments were found, and each segment follows the format given in Table I.A), where:

- I_1, I_L are identifiers of the first and last GNSS point used to describe this clothoid,
- x_0, y_0, z_0 are the XYZ coordinates of the initial point of the clothoid,

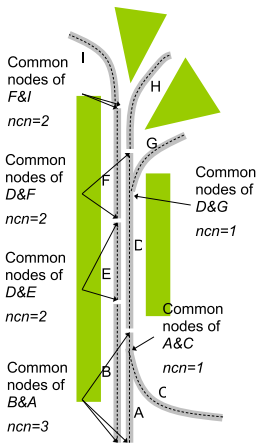

Fig. 5. Scheme representation of road segments with different cases under study on a highway. In the upper side of the image, an example of the driving direction criterion: from bottom to top the connection $F2I = 1$, while $I2F = 0$ (a displacement from I to F is not accepted). Different examples of common nodes between pairs of segments are presented, representing situations of $ncn = 1, 2$ and 3.

TABLE I

ROAD SEGMENTS FORMAT WITHOUT A) AND WITH B) CONNECTIVITY CONNECTIVITY INFORMATION.

A)

I_1	I_L	x_0	y_0	z_0	x_L	y_L	z_L	τ_0	κ_0	c_0	L

B)

Format of Table A)	NN	N1	N2	N3	...	N19

- x_L, y_L, z_L the correspondent for the last point,
- τ_0, κ_0, c_0 stand for initial yaw angle, initial curvature and its linear rate respectively, and
- L is the length of the clothoid segment.

Regarding connectivity, segments of this Emap have between 0 (for those segments that constitute the bounds of the Emap) and 7 connections, being 3 and 4 connections the most usual numbers with around 60 % of the cases. Due to the benefits of working with fixed sized arrays of data and following a conservative principle, we decided to reserve 19 fields for the identifiers of the segments connected to the one under study. This number represents a very safe estimator, while it was found that a lower number of candidates does not bring any significant reduction in terms of computation. The new format for a segment data row is shown in Table I.B). Apart from the elements already included in Table I.A), `NN` stands for the number of neighbors of the road segment in Table I.B), and `N1`, `N2`, `N3` ...`N19` are the identifiers of these neighbors, with null values for those fields unused when `NN` < 19. Following this approach, the final Emap file of Cheviré bridge was smaller than 100KB.

Next step will be dedicated to fill up the fields of identifiers for every road segment of the Emap. Since bijective relations between segments were disregarded, the application of the results obtained from one segment in the study of another does not bring any particular benefit to our algorithm. On the contrary, taking into consideration bijective relations diminishes the capability to find connected segments automatically, being this the main reason to neglect that possibility. Consequently, we follow the simple strategy of finding connected segments for only one road segment at one step, what implies the systematical repetition of the algorithm as many times as segments are in the map.

B. PRE-SELECTION OF CANDIDATES

For the sake of simplicity in the description of the algorithm, let us assume that the vehicle is at the present time in the road segment A. Our first task is to preselect possible candidates which verify that a transition from A to them would be feasible. To realize this we decided to follow a simple strategy of looking for those segments with any point closer to a certain distance to any point of segment A. The computation of this may be high, but since we do not need high precision in the value of the distance, the final process can be accomplished quickly. By taking into account the frequency of most common GPS/DR navigation systems (usually higher than 5 Hz), and vehicle and road speed limitations, a resolution value of 1 m and a distance criterion of 5 m were selected and found suitable. As a result of the pre-selection process, in the trials performed in Cheviré bridge, positive candidates were never missed, while the number of wrong positives remained typically not higher than 50% of the final connected segments.

C. DEFINITION OF COMMON NODES

Let us assume that a vehicle is in road segment A, and points A_i, A_l define respectively the initial and the last extremities of this segment. Let us assume as well that in the previous phase we found one candidate segment B, with extremities B_i, B_l. To ease the process of determining if segment B can be a future segment when moving from segment A we introduce the concept of a common node. In a traditional map definition, nodes are the extremities of the road segments, and their definition includes different properties, depending for example on whether or not this segment is connected to some others at this node. In the analysis of the relation $A2B$ proposed in this paper, a common node is an initial or a last point of A or B that is close enough to any point of the other segment. When an extremity is found to be a common node, its flag is set to 1, being the default state for the relation $A2B$: $A_i = A_l = B_i = B_l = 0$. For our experiments the threshold of proximity was established in 5 m. Fig. 5 illustrates the concept of common nodes.

D. CASES OF STUDY

According to the definition of common nodes, there are 5 possible situations in the study of $A2B$, depending on the number of common nodes between A and B, ncn_{A2B} : $\{0, 1, 2, 3, 4\}$. Next, we analyze all these cases.

1) $ncn_{A2B} = 0$: This is the case of those pairs of segments that have two points 5 m or less close, but none of their extremities is close to any point of the other segment, something never found in our experiments.

2) $ncn_{A2B} = 1$ *:* Some situations that match this value are presented in Fig. 5. The algorithm applied to determine the connection from A to B depending on the flag values is given next:

```
if (A_l = 1) OR (B_i = 1) OR
   ( (A_i = 1) AND ( Δ(A_τ0, B_τ0) < PI/2 ) )
   then ⇒ A2B = 1;
else ⇒ A2B = 0;
```

where the expression $\Delta(A_{\tau_0}, B_{\tau_0})$ represents the difference between initial road segment heading angles (in radians). The inclusion of this rule is to contemplate the case of segments with similar orientations for a stretch at the beginning of segment A, what makes possible a transition from A to B. For differences higher than 90 degrees it is assumed that it is not feasible to perform such a maneuver.

3) $ncn_{A2B} = 2$ *:* Along with the previous case, $ncn_{A2B} = 2$ represents most common situations on a multiple lane road. Some of its possible combinations are represented in Fig. 5. The rules employed to determine whether or not it is accepted as feasible to make a transition from A to B are:

```
if (A_l = 1) AND (B_l = 1) AND (dist(A_l, B_l) < 2)
   then ⇒ A2B = 0;
elseif (A_i = 1) AND (B_l = 1) AND
        (dist(A_i, B_l) < 2)
   then ⇒ A2B = 0;
elseif (A_i = 1) AND (B_i = 1) AND
        (dist(A_i, B_i) < 2) AND
        ( Δ(A_τ0, B_τ0) > PI/2)
   then ⇒ A2B = 0;
else ⇒ A2B = 1;
```

where $dist(A_i, B_i)$ stands for the Euclidean distance between these two points.

4) $ncn_{A2B} = 3$ *or* $ncn_{A2B} = 4$*:* In these cases, 3 or 4 of the 4 possible nodes of A and B are close to at least one point of the other segment, what corresponds to the case of parallel segments than start or finish in very close points (Fig. 5). For these cases it will be accepted that $A2B = 1$ without further considerations.

E. RESULTS AND FURTHER CONSIDERATIONS

The result of applying this algorithm has been verified for the Emap under consideration. To the best of our knowledge, among the 553 segments and 1694 links of Cheviré bridge Emap, only one connection was not automatically found. The case corresponded to $ncn_{A2B} = 1$ in which $B_l = 1$. In this very concrete case, a practical reasoning gives an idea of the consequences of this connection gap. The problematic segment has a length of 49 m. By visual inspection it can be observed that it is not feasible to make the mismatched transition during a stretch of approximately 20 m. Therefore, assuming that a vehicle travels in this area (with a speed limit of 90 km/h) at 72 km/h (20 m/s) this would have approximately 1.5 s to perform a complete lane change, leave the bounds of the original segment, and enter in the new segment. Since a standard lane change on a highway road takes around 3 s, it can be accepted that this situation will not appear often in real traffic circumstances. Nonetheless, the wrong connection of the lane segment was corrected manually. As a conclusion to this, a posterior revision and analysis of the connections is advisable.

VI. CONCLUSIONS AND FUTURE WORKS

Mobile mapping was used for data collection and Emap computation in the frame of this research. Emap, for Enhanced map, is based on a geometrical representation of each road lane with series of clothoids: an EKF processes the smoothed GPS and dead-reckoning vehicle trajectory. Maximum deviation between the extracted geometry and the vehicle location was bounded to 5 cm. An automated algorithm was programmed to determine the connectivity relations among segments of the Emap. This algorithm was applied to the Cheviré bridge Emap presenting very good results, and with low computational time. Nevertheless, it is recommended to verify the connections between segments in those specific cases that may be not considered by the current algorithm. The resulting Emap was satisfactorily applied to a combined fusion/map-matching algorithm that meets the requirements of ITS applications for positioning and mapping at lane level accuracy. Future works in this topic focus on further improvement of the extraction process, where one would not fix the initial coordinates of the clothoids, but let it be identified as additional state variables of the filter. In addition to that, more complex rules that take into account singular connectivity cases are under development.

ACKNOWLEDGMENTS

This investigation has been carried out in the frame of the European project CVIS (Cooperative Vehicle Infrastructure Systems) by researchers of LCPC (Geo localization Division) and UTC (Heudyasic Lab), both partners of the Positioning and Mapping subproject POMA of CVIS, and the group of Intelligent Systems/University of Murcia, awarded as an excellence researching group in frames of the Spanish Plan de Ciencia y Tecnología de la Región de Murcia.

REFERENCES

[1] Quddus, M.A., Ochieng W.Y. Noland R.B., *Current map-matching algorithms for transport applications: State-of-the-art and future research directions*. Elsevier Transportation Research Part C, 15, pp. 312–328, 2007.

[2] Wang J., Shroedl S., Mezger K., Ortloff R., Joos A., Passegger T., *Lane Keeping Based on Location Technology*. IEEE Transactions On Intelligent Transportation Systems, Vol. 6, No. 3, 351–356, 2005.

[3] Shroedl S., Rogers S., Wilson C., *Map refinement from GPS traces*. DaimlerChrysler Res. and Technol. North America, Palo Alto, CA, RTC Rep. No. 2000/6, 2000.

[4] Eidehall A., Pohl J. and Gustafsson F., *Joint road geometry estimation and vehicle tracking*. In Proceedings of the IEEE Intelligent Vehicles Symposium 2004, pages 619–624, 2004.

[5] Bétaille D., *GYROLIS: logiciel de localisation de véhicule en post-traitement par couplage GPS-gyromètre-odomètre*. Bulletin Spécial Instrumentation des Laboratoires de Ponts et Chaussées, No 275, 2008.